

AD-A275 170

Identification of an Unexpected Space Radiation Hazard

1 November 1993

Prepared by

J. B. BLAKE
Space and Environment Technology Center
Technology Operations
The Aerospace Corporation
El Segundo, CA 90003

M. S. GUSSENHOVEN AND E. G. MULLEN
Phillips Laboratory/GPSP
Hanscom AFB, MA 10731

R. W. Fillius
University of California, San Diego
La Jolla, CA 92093

DTIC
ELECTE
FEB 01 1994
S E D

Prepared for

SPACE AND MISSILE SYSTEMS CENTER
AIR FORCE MATERIEL COMMAND
2430 E. El Segundo Boulevard
Los Angeles Air Force Base, CA 90245

Engineering and Technology Group

APPROVED FOR PUBLIC RELEASE;
DISTRIBUTION UNLIMITED

280 94-03157



**THE AEROSPACE
CORPORATION**
Segundo, California

94 1 31 241

This report was submitted by The Aerospace Corporation, El Segundo, CA 90245-4691, under Contract No. F04701-88-C-0089 with the Space and Missile Systems Center, 2430 E. El Segundo Blvd., Los Angeles Air Force Base, CA 90245. It was reviewed and approved for The Aerospace Corporation by A. B. Christensen, Principal Director, Space and Environment Technology Center. Capt. Leslie Belsma was the project officer for the Mission-Oriented Investigation and Experimentation (MOIE) program.

This report has been reviewed by the Public Affairs Office (PAS) and is releasable to the National Technical Information Service (NTIS). At NTIS, it will be available to the general public, including foreign nationals.

This technical report has been reviewed and is approved for publication. Publication of this report does not constitute Air Force approval of the report's findings or conclusions. It is published only for the exchange and stimulation of ideas.

Leslie E. Belsma

Capt. Leslie Belsma, Captain USAF
Project Officer

Wm. Kyle Sneddon

Wm. Kyle Sneddon, Captain USAF
Deputy, Industrial & International Division

Accession For	
NTIS	CRA&I <input checked="" type="checkbox"/>
DTIC	TAB <input type="checkbox"/>
Unprocessed	<input type="checkbox"/>
Distribution	
By	
Distribution	
Availability Codes	
Dist	Avail and/or Special
A-1	

REPORT DOCUMENTATION PAGE			Form Approved OMB No. 0704-0168	
Public reporting burden for this collection of information is estimated to average 1 hour per response, including the time for reviewing instructions, searching existing data sources, gathering and maintaining the data needed, and completing and reviewing the collection of information. Send comments regarding this burden estimate or any other aspect of this collection of information, including suggestions for reducing this burden to Washington Headquarters Services, Directorate for Information Operations and Reports, 1215 Jefferson Davis Highway, Suite 1204, Arlington, VA 22202-4302, and to the Office of Management and Budget, Paperwork Reduction Project (0704-0168), Washington, DC 20503.				
1. AGENCY USE ONLY (Leave blank)		2. REPORT DATE 1 November 1993		3. REPORT TYPE AND DATES COVERED
4. TITLE AND SUBTITLE Identification of an Unexpected Space Radiation Hazard			5. FUNDING NUMBERS F04701-88-C-0089	
6. AUTHOR(S) Blake, J. B.; Gussenhoven, M. S.; Mullen, E. G.; and Fillius, R. W.				
7. PERFORMING ORGANIZATION NAME(S) AND ADDRESS(ES) The Aerospace Corporation Technology Operations El Segundo, CA 90245-4691			8. PERFORMING ORGANIZATION REPORT NUMBER TR-92(2940)-12	
9. SPONSORING/MONITORING AGENCY NAME(S) AND ADDRESS(ES) Space and Missile Systems Center Air Force Materiel Command 2430 E. El Segundo Boulevard Los Angeles Air Force Base, CA 90245			10. SPONSORING/MONITORING AGENCY REPORT NUMBER SMC-TR-93-60	
11. SUPPLEMENTARY NOTES				
12a. DISTRIBUTION/AVAILABILITY STATEMENT Approved for public release; distribution unlimited			12b. DISTRIBUTION CODE	
13. ABSTRACT (Maximum 200 words) A new radiation belt was formed on 24 March 1991 by the interaction of a strong shock in the solar wind with the Earth's magnetosphere. This brief report describes observations of the moment of creation by sensors aboard the CRRES (Combined Release and Radiation Effects Satellite).				
14. SUBJECT TERMS CRRES mission, ultra-relativistic electrons in radiation belts, new radiation belt			15. NUMBER OF PAGES 4	
			16. PRICE CODE	
17. SECURITY CLASSIFICATION OF REPORT UNCLASSIFIED	18. SECURITY CLASSIFICATION OF THIS PAGE UNCLASSIFIED	19. SECURITY CLASSIFICATION OF ABSTRACT UNCLASSIFIED	20. LIMITATION OF ABSTRACT	

Identification of an Unexpected Space Radiation Hazard

J. B. Blake¹, M.S. Gussenhoven², E.G. Mullen², and R.W. Fillius³

Abstract

A new radiation belt was formed on 24 March 1991 by the interaction of a strong shock in the solar wind with the Earth's magnetosphere. This brief report describes observations of the moment of creation by sensors aboard the CRRES (Combined Release and Radiation Effects Satellite).

I. INTRODUCTION

On 22 March 1991 at 22:47 UT an X-ray event and a 3B optical flare were observed on the Sun. These occurrences were followed almost four hours later by another solar X-ray event. Energetic particles, both ions and electrons, began to arrive in the vicinity of the Earth about 0730 UT on 23 March. These particles were followed by the arrival of a strong shock in the solar wind at the Earth at 03:42 UT on 24 March, presumably from the solar-flare events mentioned above, although this assignment is not certain. Almost immediately following arrival of the shock, sensors aboard CRRES (Combined Release and Radiation Effects Satellite) observed the injection of protons and electrons with energies of 10s of MeV to form a new radiation belt between the well-known Inner Zone and Outer Zone.

The energies and intensities of the newly-injected particles were such that they greatly increased the radiation dose received by a spacecraft in the region of space occupied by the new radiation belt. The purpose of this paper is to describe how the content of this new radiation belt was determined.

II. SATELLITE AND INSTRUMENTATION

The CRRES satellite was launched on 25 July 1990 into an orbit with an apogee of 33,575 km, a perigee of 323 km, and an inclination of 18.2°. The observations discussed in this paper were made with four different sensors.

One of these sensors was nearly identical to that flown as part of the University of California, San Diego (UCSD) complement aboard Pioneer 10 and Pioneer 11 by Fillius and McIlwain [1], a Cerenkov counter employing a water-methanol radiator. A photomultiplier detected the optical radiation (Cerenkov light) emitted by a particle that exceeded the speed of light in the radiator. (Recall that the speed of light is a function of the index of refraction of the medium, about 1.28 in water-methanol). The three nominal energy thresholds were > 6 MeV, > 9 MeV, and > 13 MeV for electrons. The proton

energy thresholds were hundreds of MeV. The Cerenkov counter had directional sensitivity. In the following for convenience, we will refer to the Cerenkov channels by their electron thresholds.

The second and third sensors consisted of single, shielded silicon detectors. The sensors were described by Blake and Imamoto [2]. The two shields required protons to have 20 MeV and 50 MeV, respectively, to penetrate, and the electronic thresholds were set high enough to ensure that there was no sensitivity to electrons of any energy. The nominal proton energy channels were 20 to 80 MeV and 50 to 110 MeV.

The fifth sensor was a telescope consisting of a stack of 6 silicon detectors. There were 16 energy channels from 6 to 100 MeV. The instrument is discussed in detail by Violet et al. [3].

III. OBSERVATIONS AND DISCUSSION

Figure 1 shows the countrate in the $e > 6$ MeV and p 20 to 80 channels as a function of time as CRRES moved inbound at a distance from the surface of the Earth of approximately $1.65 R_E$ ($L \approx 1.65$). The plot begins just prior to arrival of the shock at the Earth. The countrate is low in both channels as would be expected in the region between the Inner Zone and Outer Zone. This region is often referred to as the Slot Region for obvious reasons. Abruptly, both channels show orders-of-magnitude increases in countrate as well a strange,

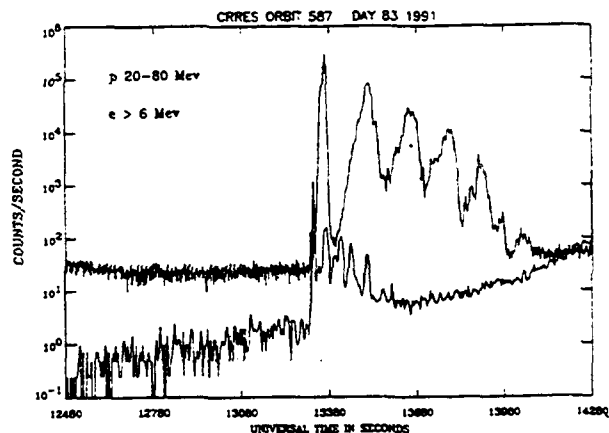


Figure 1. A plot of the countrate in the 20 to 80 MeV and $e > 6$ MeV channels as CRRES moved inbound during the time period of the arrival of the strong shock in the solar wind. The enormous increases in countrate occurred within approximately one minute of the arrival of the shock at the boundary of the magnetosphere. The electron channel saturated the counter in the data system. The actual countrate exceeded 10^6 per second.

"picket fence" structure. In fact, the first peak in the electron channel would be an order of magnitude larger except that its scaler has rolled over. Subsequently, CRRES moves below an altitude of $1.0 R_E$ ($L = 2$) and out of the region of newly injected particles.

The interpretation of the structure is outlined in Figure 2, which is a cartoon of the event. If particles are injected in an

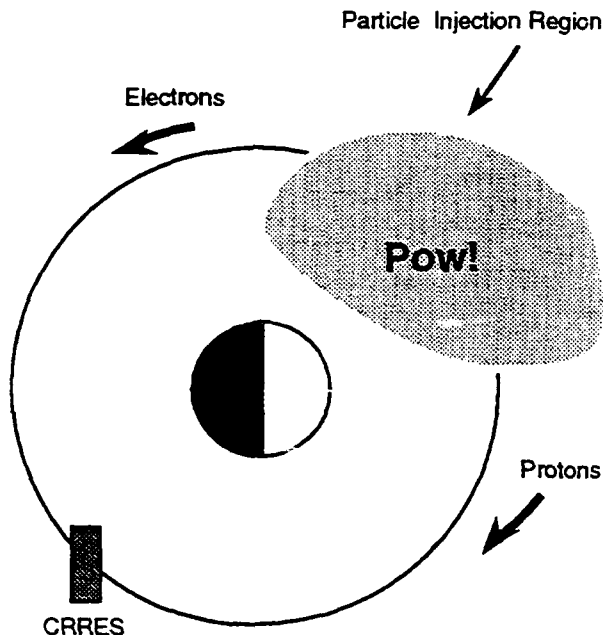


Figure 2. A cartoon of the injection event. The positive and negative particles move around the Earth in opposite directions and, as they move, they spread out because of differing energy and particle identity.

apparently localized region in the Earth's magnetosphere, they will move in packets around the Earth, repeatedly passing the observer. Because the drift speed is energy-dependent, the particles spread out in longitude with time. In the scientific literature, these packets are referred to as "drift echoes." Figure 3 shows the count rate in a relatively narrow, differential energy channel in the proton telescope. The separation of the peaks is in excellent agreement with that calculated for a proton energy of 29 MeV. This agreement gives confidence in the interpretation of the count rate structure as drift echoes. Figure 4 shows the count rate for an integral electron channel, $e > 6$ MeV. The count rate vs time in this counter is very different than that from the proton counter plotted in Figure 3. This difference is due to the fact that the electron detector has an integral response with a uniform efficiency above 6 MeV. The "sawtooth" in the count rate vs time is a measure of the energy spectrum; the lower energy but more abundant electrons arrive later. As indicated in Figure 4, a peak in the flux occurs at 15 MeV; at lower energies the flux decreases. The Earth's magnetic field acted as a giant magnetic spectrometer, permitting a

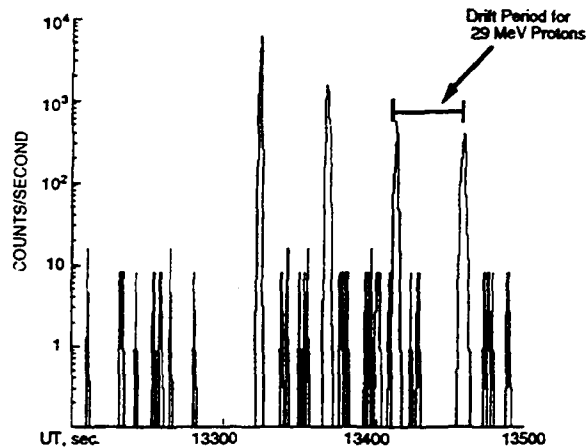


Figure 3. A plot of the count rate vs time in a relatively narrow proton channel 26 - 36 MeV. The characteristic "picket fence" of a drift echo is clearly seen. The separation in time is an unambiguous measure of the proton energy.

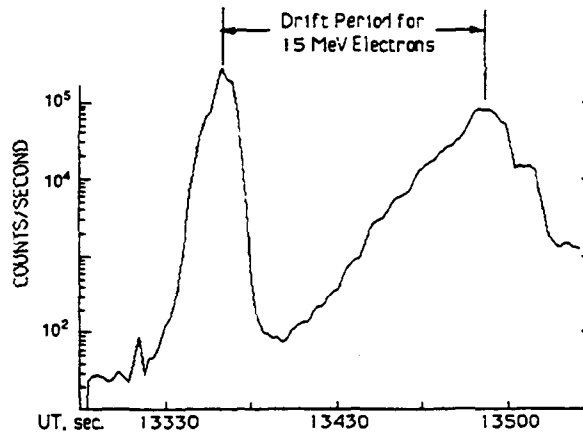


Figure 4. A plot of the count rate vs time in an integral electron channel, $e > 6$ MeV. Because the detector is measuring particles with a broad spectrum of energies, the profile is a ramp rather than narrow peaks.

detailed measurement of the particle energy spectra. These measurements allowed us to accurately determine the electron energy spectrum in the new radiation. Without these fortuitous observations, such a determination would have been impossible. Since the presence of electrons in the Earth's radiation belts with energies from 15 MeV to greater than 50 MeV was completely unexpected, no sensor was on board capable of spectral measurements in this energy range.

It is most informative to examine the radial profiles of the sensor counting rates as a function of radial distance. (In this

plot, the radial profile is labeled by L . The L value is the radial distance of the equatorial crossing of a magnetic field line from the Earth's center. Figure 5 displays the radial profiles two days before the injection event, two days after the event, and six months after the injection event for the 20 to 80 MeV proton channel and the third Cerenkov channel, nominally > 13 MeV electrons.

In the top panel, which gives the "before" profile, the 20 to 80 MeV Inner-Zone proton count rate shows a broad peak near $L = 1.5$. Outside of $L = 2$, the proton intensity is much less and decreases to a background rate due to Galactic cosmic rays near $L = 3$. The Cerenkov counter channel shows a small peak inside $L = 2$, which is due to protons with energies of several hundred MeV. Outside of $L = 2$, this channel is at the background rate due to Galactic cosmic rays.

The middle panel shows the dramatic change in the particle population that resulted from the injection event. A second proton peak has appeared at a higher altitude with a relative minimum between the original one and the newly injected particles. The Cerenkov channel shows a larger change; between L of 2 to 4, its count rate is orders of magnitude above the rate shown in the top panel in the same region of the magnetosphere. In this region the count rate is due to electrons with energies > 13 MeV, not relativistic protons as is the case inside of $L = 2$. The "thick" count rate curve around the peak intensity results from the fact that the electron flux depended upon the angle between the electron velocity vector and the ambient magnetic field. The Cerenkov counter was scanned by the spinning CRRES spacecraft, and all pitch angles are shown in the plot.

The third panel shows that the intensities of the new particles had decreased over the six-month period following the injection event, and the spatial location of the peaks had moved to a lower altitude. The intensity dependence of the electrons upon pitch angle had decreased.

IV. CONCLUSIONS

The electrons and protons injected into the Earth's magnetosphere in this event are highly penetrating and represent a threat to spacecraft orbiting in that region of near-Earth space. The dramatic increase in radiation dose is described by Gussenhoven et al. [4]. The injection event was completely unexpected and may have been a unique occurrence in magnitude during 35 years of space research. However, the response of the early particle sensors to such an event is not obvious, therefore a definitive conclusion is difficult to make. The formation, evolution, and decay of the high-energy-electron belt is now being addressed. The decay of the new radiation belt is complex. It is clear that further understanding of radiation belt processes is needed for the design of space systems.

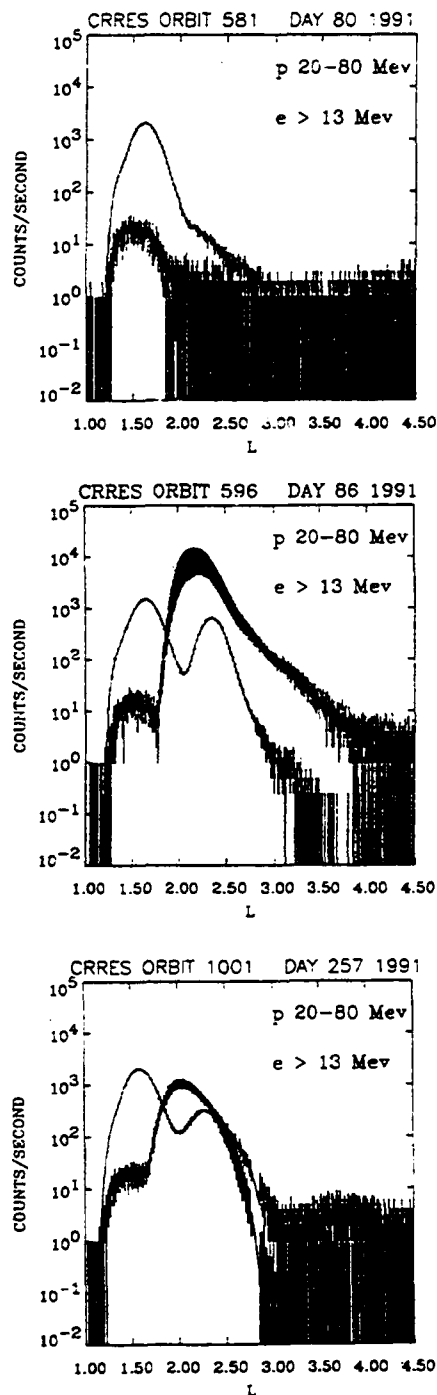


Figure 5. The three panels show the radial profiles for the 20 to 80 MeV proton channel and the $e > 13$ MeV electron channel for an orbit just before the injection event, just afterwards, and six months afterwards. The major change in the energetic particle population caused by the injection event and the evolution of the particle population with time can be seen.

V. ACKNOWLEDGEMENTS

This work was supported at The Aerospace Corporation under Air Force Space Systems Division Contract FO4701-88-C-0089.

VI. REFERENCES

- [1] R.W. Fillius and C.E. McIlwain, "Measurements of the Jovian Radiation Belts," *J. Geophys. Res.*, Vol. 89, p. 359, 1974.
- [2] J.B. Blake and S.S. Imamoto, "The Proton Switches," *J. of Spacecraft and Rockets*, in press, 1992.
- [3] M.D. Violet, K. Lynch, R. Redus, K. Riehl, E. Boughan, and C. Hein, "The Proton Telescope (PROTEL) on the CRRES Spacecraft," *IEEE Trans. Nuc. Sci.*, submitted, 1992.
- [4] M.S. Gussenhoven, E.G. Mullen, Michele Sperry, J.B. Blake, and C.E. Jordan, "The Effect of the March 1991 Storm on Accumulated Dose for Selected Satellite Orbits: CRRES Dose Models," *IEEE Trans. Nuc. Sci.*, this issue.

TECHNOLOGY OPERATIONS

The Aerospace Corporation functions as an "architect-engineer" for national security programs, specializing in advanced military space systems. The Corporation's Technology Operations supports the effective and timely development and operation of national security systems through scientific research and the application of advanced technology. Vital to the success of the Corporation is the technical staff's wide-ranging expertise and its ability to stay abreast of new technological developments and program support issues associated with rapidly evolving space systems. Contributing capabilities are provided by these individual Technology Centers:

Electronics Technology Center: Microelectronics, solid-state device physics, VLSI reliability, compound semiconductors, radiation hardening, data storage technologies, infrared detector devices and testing; electro-optics, quantum electronics, solid-state lasers, optical propagation and communications; cw and pulsed chemical laser development, optical resonators, beam control, atmospheric propagation, and laser effects and countermeasures; atomic frequency standards, applied laser spectroscopy, laser chemistry, laser optoelectronics, phase conjugation and coherent imaging, solar cell physics, battery electrochemistry, battery testing and evaluation.

Mechanics and Materials Technology Center: Evaluation and characterization of new materials: metals, alloys, ceramics, polymers and their composites, and new forms of carbon; development and analysis of thin films and deposition techniques; nondestructive evaluation, component failure analysis and reliability; fracture mechanics and stress corrosion; development and evaluation of hardened components; analysis and evaluation of materials at cryogenic and elevated temperatures; launch vehicle and reentry fluid mechanics, heat transfer and flight dynamics; chemical and electric propulsion; spacecraft structural mechanics, spacecraft survivability and vulnerability assessment; contamination, thermal and structural control; high temperature thermomechanics, gas kinetics and radiation; lubrication and surface phenomena.

Space and Environment Technology Center: Magnetospheric, auroral and cosmic ray physics, wave-particle interactions, magnetospheric plasma waves; atmospheric and ionospheric physics, density and composition of the upper atmosphere, remote sensing using atmospheric radiation; solar physics, infrared astronomy, infrared signature analysis; effects of solar activity, magnetic storms and nuclear explosions on the earth's atmosphere, ionosphere and magnetosphere; effects of electromagnetic and particulate radiations on space systems; space instrumentation; propellant chemistry, chemical dynamics, environmental chemistry, trace detection; atmospheric chemical reactions, atmospheric optics, light scattering, state-specific chemical reactions and radiative signatures of missile plumes, and sensor out-of-field-of-view rejection.